Green Corrosion Inhibition studies in mild steel using *Mukia maderaspatana* plant extracts

Vinayagam Rajasekar[*a], Moorthy Shyamala[b], Jeyaseelan Aravind[c]

[1]*Department of Industrial Biotechnology, Government College of Technology, Coimbatore-641013, Tamilnadu, India. ORCID: 0009-0007-9940-8047*

[2]*Department of Chemistry, Government College of Technology, Coimbatore-641013, Tamilnadu, India. ORCID: 0009-0007-4018-8625*

[3]*Department of Biotechnology, Saveetha School of Engineering, Saveetha Institute of Medical and Technical Sciences, Saveetha University, Chennai, India. ORCID: 0000-0001-9699-2312*

***Corresponding author:** Vinayagam Rajasekar,

Corresponding author Email id: rajasekar@gct.ac.in; rajasekaribtgct@gmail.com

Abstract

Using green corrosion inhibitors, which lower corrosion rates without endangering the environment, is one of the most important strategies for reducing corrosion. An extract from the leaf of the *Mukia maderaspatana* plant was used in this investigation as a green corrosion inhibitor for mild steel in hydrochloric acid. The anti-corrosion properties of plant leaf extract were verified by a number of experimental procedures, such as weight loss analysis, electrochemical spectroscopy, gravimetric measurements and surface analysis using FTIR, and SEM, at various temperatures. A plant extract added at 1000 ppm significantly increases the inhibitory effectiveness up to a maximum of 95%. To confirm that the mild steel surface in an HCl solution had a protective layer, surface analysis was done. An investigate using a scanning electron microscope showed that the protective layer formed by the green inhibitor. According to the study, the extract from *Mukia maderaspatana* is a strong, environmentally friendly inhibitor that efficiently stops mild steel from corroding in extremely acidic situations.

Keywords: Green method; corrosion inhibition; plant extract; electrochemical spectroscopy; Surface analysis

Introduction

Low carbon steel is a highly sought-after steel-related material, utilized in a variety of sectors from heavy machinery to agricultural, due to its exceptional toughness and flexibility, as well as its relatively low manufacturing costs. In spite of this, it is extremely vulnerable to corrosion in acidic conditions during industrial procedures, such as washing equipment with

metal surfaces. Because of its erosive properties and affordable price, hydrochloric acid is the mineral acid that is most frequently used in industrial operations. But frequent use of this acid causes mild steel to corrode, which compromises the metal's integrity [1-4]. The degradation of a material when it comes into touch with the environment is known as corrosion of steel alloy. Diffusion-controlled development of oxygen caused an oxide coating to be formed on the metal surface. These might accelerate the metal's oxidation. Aqueous corrosion can happen in damp environments because of electrochemical processes. This can be stopped by putting corrosion inhibitors in the acid, which forms a protective layer on the metal surface through the inhibitor's adsorption and inhibits direct communication between the metal and the acid [5-8].

Literature research has shown that while synthetic inhibitors are very efficient, many are hazardous and harm the environment and humans. Green inhibitors are ecologically friendly, unlike these inhibitors. Green inhibitors are environmentally safe, non-toxic, and can be broken down naturally. Plant extracts are a bountiful supply of naturally occurring chemical compounds that may be acquired inexpensively through straightforward methods. Researchers discovered that green inhibitors effectively adhere to the metal surface, making them suitable corrosion inhibitors; this is attributed to functional groups with hetero atoms (O, N, S, and P). Corrosion inhibitors stick effectively to the metal surface contact and create an extended biofilm with the assistance of functional groups, including hetero atoms, π-electrons, and aromatic rings, enhancing corrosion inhibition. Researchers have said that utilizing plant extracts as inhibitors in an acidic environment is helpful [9-12]. Some authentications from previous observations. Krishnaveni et al.[13] experimented using *Morinda tinctoria* leaf extract as green inhibitors on mild steel in an acid medium. Anti-corrosion behaviour was studied using weight loss studies, colorimetric estimation, Electrochemical studies (EIS), and Scanning electron microscope (SEM), and it was found that the inhibitor attained more efficiency under room temperature. The effect of temperature studies showed that an increase in temperature decreases the inhibition efficiency, and the maximum IE was 93.83%. Electrochemical studies indicated that colorimetric results fit well with weight loss analysis, and polarization studies indicated the mixed nature of inhibitors. Mobin et al.[14] studied the anti-corrosion behavior of bromelain (pineapple stem extract) on low-carbon steel in 1M HCl solution using EIS, UV vis spectrometry, potentiodynamic polarization studies, SEM, and the results obtained suggested that bromelain acted as a suitable corrosion inhibitor. The highest inhibition efficiency was 97.6% for the extract concentration of 1000 ppm at 338°K. From EIS studies, they concluded that inhibitor

adsorption on mild steel follows Langmuir adsorption isotherm. Also, potentiodynamic polarization studies proclaimed that *Mukia maderasapatna* behaved as a mixed-type inhibitor and controlled both the announcement and cathodic processes. Figure 1 a and 1b show the research trend on using plant extract as corrosion inhibitor all various metals including mild steel.

The adsorption of inhibitor molecules on mild steel is associated to a reduction in the double-layer resistance (C_{dl}) and an increase in the charge transfer resistance (R_{ct}) when *Mukia maderasapatna* is added to an acidic solution, according to an investigation conducted using electrochemical impedance spectroscopy (EIS). SEM observations revealed that the inhibited steel had a smoother surface morphology and less corrosion, suggesting the formation of a protective layer. Using weight loss and electrochemical methods, Fourier-transform infrared spectroscopy (FTIR), UV-visible spectrometer, quantum chemical analysis, and scanning electron microscopy (SEM), Li et al. [15] investigated the inhibitory effect of radish leaf extract on mild steel corrosion in 0.5M H_2SO_4. The study on the effect of temperature revealed that the inhibitory effectiveness decreased with rising temperatures and increased with greater concentrations of RLE. At a concentration of 300 mg/L of RLE, the greatest ionization efficiency of 93% was achieved at 298 Kelvin. The inhibitor adsorption on mild steel showed features of a mixed-type inhibitor, according to studies on EIS and adsorption isotherms. The research observes that both chemical and physical adsorption occur simultaneously and follows Langmuir's adsorption isotherm. Al Otaibi et al.[16] investigated the electrochemical characteristics of carbon steel in a 0.25M H_2SO_4 solution in order to assess the efficacy of the extract. Electrochemical Impedance Spectroscopy (EIS) studies at a concentration of 283.4 ppm demonstrated an inhibitory effectiveness of 98%. The extract stuck to the Langmuir adsorption isotherm and acted as a cathodic inhibitor, as demonstrated by the polarization curves.

The presented work deals with the corrosion inhibition properties of *Mukia maderaspatana* plant leaf extract, and this plant belongs to the kingdom plantae of the division Dermatophytes, sub-division Angiospermae of class Dicotyledonae, subclass polypetalae of series Calyiflorae, order passiflorae, family Cucurbitaceae of the Genus Mukia.This plant aggressively grows in India and Sri Lanka.In Tamil Nadu,it is regionally called Mosumosukai or musumusukkai, whose English name is Madras pea pumpkin or Rough bryony.Its leaves are symmetrically ovate,have 3 to 5 lobes,and are 3-9 cm long. The leaves of the *M.maderapatana* are composed of 4 – methylpentyl ester, 4-methoxy,butyn-1-ol,dichloroacetic acid, and other components such as carbohydrates, steroids, tannins, and

flavonoids [17].*Mukia maderaspatana* could be a promising source for plant extract corrosion inhibitors.

The current study aims to investigate the anti-corrosion properties of MME on low-carbon steel in a 1M HCl solution. EIS, adsorption isotherm, and potentiodynamic methods are employed to investigate corrosion inhibition processes and analyze the creation of the protective layer on low-carbon steel throughout the corrosion process using scanning electron microscopy, FTIR, visible UV spectroscopy, and quantum chemical analysis.

2. Experimental Methods

2.1. *Mukia maderaspatana* plant extract segregation

The extract was prepared from leaves of the *Mukia maderaspatana* plant, which was gathered in Coimbatore, Tamilnadu, India. After being washed with tap water to remove any undesired impurities, the leaves were allowed to air dry. To obtain the kernel powder, muslin cloth was used to filter aqueous leaf powder extracts, and the supernatant was then dried. Using the method described by Krishnaveni et al. [13], crude PE was prepared using 25g of MME powder.

2.2. Mild steel specimen preparation

The chemical composition of the mild steel under investigation in this study was C (0.07%), Mn (1.20%), Si (0.40%), P (0.01%), Cu (0.04%), Al (0.05%), and Cr (0.12%), with Fe making up the remaining weight percentage. For weight loss and electrochemical investigations, coupons made of mild steel, rectangular in shape and measuring 1 × 5 × 0.2 cm, as well as square coupons with a surface area of 1 cm^2 and a thickness of 0.2 cm, were utilized. The item was utilized for a weight loss research after being polished using different-grade emery sheets, degreased with acetone, cleaned with distilled water, and dried [13].

2.3 Gravimetric measurements

After recording the initial weight of the coupons, 100 milliliters of 1M HCl solution containing and excluding MME concentration (200 –1000 ppm) was added, and the metal pieces were left to sit for 3, 6, 12, 24, 48 hours, and at temperatures of 303, 308, 313, 318, 323, 328, and 333 K, respectively. The coupons were then dried, desiccated, and reweighed after being washed with water and acetone [18]. Using the following formulas, the corrosion rate (mmpy), inhibition efficiency (IE), and surface coverage (θ) were calculated from the mass loss using Eqs. 1 to 3 [19, 20].

$$\text{Corrosion (mmpy)} = \frac{87.6 \times \text{weight loss (mg)}}{\text{density}\left(\frac{\text{g}}{\text{cc}}\right) \times \text{Area}\left(\text{cm}^2\right) \times \text{Time}\left(\text{h}\right)} \quad (1)$$

$$\text{Inhibition efficiency (\%)} = \frac{CR_0 - CR_i}{CR_0} \times 100 \quad (2)$$

$$\text{Surface Coverage } (\theta) = \frac{CR_0 - CR_i}{CR_0} \times 100 \quad (3)$$

Where CR_0 and CR_i rare corrosion rate in the absence and presence of the inhibitor.

2.4. Electrochemical measurements

Electrochemical experiments were conducted using potentiodynamic polarization, where the electrode's potential is altered at a chosen rate by delivering current through the electrolyte. The electrodes used in this approach are (1) platinum electrode as the counter electrode, (2) saturated calomel electrode as the reference electrode, and (3) metal coupon as the working electrode. Experiments were conducted after immersing for 30 minutes to achieve open circuit potential. The open circuit potentials were maintained to achieve a steady-state potential. The potentiodynamic polarization test automatically varied the electrode potential from -0.1V to 1V at a scan rate of 0.5 mV s^{-1}. Impedance measurements were conducted at open circuit potential within 100 kHz to 10mHz with a 25 peak-to-peak amplitude. The inhibition percentage is calculated from charge transfer resistance values by applying the following Eq. 4 [21]:

$$\eta(\%) = \frac{R_{ct} - R_{ct_0}}{R_{ct}} \quad (4)$$

Where R_{ct_0} and R_{ct} are the charge transfer resistance with and without inhibitors, respectively.

2.5. Surface analysis

A UV-visible spectroscopic analysis was conducted on a 600 ppm MME solution in 1M HCl before and after immersing MS for 6 hours at 35°C. The systronics117model spectrophotometer was used to verify the development of the Fe^{2+} - MME complex in the 1M HCl solution. The inhibitor created a layer on the coupon surface, then dried. The resulting powder was examined using FTIR spectroscopy (Perkin Elmer) with the KBr pellet technique. The study investigated the surface structure of a mild steel sample after being

submerged in 1M HCl for 12 hours with and without the presence of 600 ppm MME. The sample was dried and then examined with a scanning electron microscope at a magnification of 20kV after the immersion period [22, 23].

2.6. Quantum chemical calculations

The density functional theory (DFT) method was a classical statistical method used to investigate the properties of many body systems, such as interacting molecules, macromolecules, and nanomaterials. Likewise, the interaction between MME constituents and metal surfaces was analyzed. Gaussian 03 programs utilize the structure of molecules, spectroscopic data, fundamental laws of quantum mechanics to predict energies, and more advanced calculations. It was employed for calculation of all quantum chemical parameters such as energy of lowest unoccupied molecular orbital (E_{LUMO}), energy of highest occupied molecular orbital (E_{HOMO}), energy gap ($\Delta E_{LUMO-HOMO}$), absolute electronegativity (χ), dipole moment (μ), global hardness (η), electron affinity(A), ionization potential(I), absolute softness (σ), total energy (TE), and the fraction of electrons transferred from the inhibitor to iron surface (ΔN) study the MME adsorption on the mild steel surface [24].

2.7. Mechanism of Corrosion Inhibition

The low pH of the pickling process lowers the IE of the metal surface, thus inducing the oxidation reaction by the water molecule, which is in a dipole state. The plant extract also induces a dipole moment, resulting in the surface adhesion of PE molecular side chains to the metal surface. This thin film is formed by secondary bonding interactions of PE molecular side chains through the excitement of P orbital electrons to d orbital, resulting in increased negative charge and attraction to the electron affinity of the metal ions on the surface. This process replaces the solvent molecules adhered to the metal surface with the higher affinity PE molecules and lowers the IE of metal molecules on the surface.

Lowering the IE potential difference mitigates the reactivity rate of metal molecules with the solvent molecules. The accumulation of ions on the metal surface is also reduced by the saturation of the same excess of ions from the PE by specific adsorption, also known as contact adsorption. The relative concentration of PE in the solution plays a vital role in the adsorption of anions by the positively charged metal surface. Excess ions present on the

surface than the applied potential either repels or inert the solvent molecules' oxidizing ability.

The PE contains different heteroatoms with variable electrochemical potential and IE; hence, chemisorption and physisorption occur. The chemisorption takes closer to the surface by the interaction of the π-electrons of the aromatic/heterocyclic ring and vacant d-orbitals of surface iron and hence reduces the free binding sites for solvent molecules and also the further multilayer deposition of PE by physisorption increase the free charge ions of side chain molecules on the surface of metal which repels the solvent molecules by electrostatic force. The synergy between metal surface and PE is due to different polysaccharides and other secondary metabolites [25].

3. Results and discussion

3.1. Gravimetric measurements

The corrosion rate and inhibition efficiency were evaluated using the formula provided by Mobin and Rizvi [18] and Deyab et al. [19]. The study on inhibitor efficiency in mild steel corrosion showed that the green inhibitor's effectiveness increases as the concentration of MME rises; this leads to a decrease in corrosion rate due to MME adsorption on the metal surface, forming a protective film. An investigation shows that a higher concentration, namely 1000 ppm of MME, effectively inhibits corrosion across different temperatures and immersion durations. The ionization efficiency (IE) at various temperatures (303 °K, 308 °K, 313 °K, 318 °K, 323 °K, 328 °K, and 333 °K) was measured to be 89%, 94.9%, 90%, 77%, 76%, and 59% respectively. The IE during the interaction between MME and MS varied at 90%, 82%, 76%, 72%, and 70% during contact periods of 3h, 6h, 12h, 24h, and 48h, respectively. The corrosion inhibition effectiveness was high when 1000 ppm of MME was used at 308° K for 3 hours. Moreover, there was no significant rise in inhibitory efficiency, indicating that 1000 ppm is the most effective concentration for mild steel. The current experiment demonstrates the inhibitory effect of MME in 1M HCl, as shown by Hegazy and Atlam [26] and Alkhathlanet al [27]. It was noted that when the temperature rose from 303K to 328K, the inhibitory effect diminished significantly due to a shift in equilibrium from the adsorption of MME to its desorption from the MS in the experiment.

The inhibition efficiency of the mild steel specimens studied decreased as the temperature increased. Higher temperatures result in reduced inhibitory efficiency. More hydrogen evolution from metal dissolution in an acidic solution accelerates metal corrosion. The study indicates a direct correlation between corrosion rate and immersion time.

Extending the immersion time enhances the period during which organic molecules are in contact with the solution, leading to their degradation [28].

An increase in MME content resulted in a decrease in corrosion rate. An increase in the concentration of PE leads to a rise in the variety of organic molecules available to create a complex with iron and inhibitor compounds.

3.1.1. Effect of temperature

An investigation was conducted to determine how temperature affects the anti-corrosive efficacy of the MME extract. Weight loss tests were conducted for 3 hours with inhibitor doses ranging from 200 to 1000 ppm at temperatures varying from 303 to 333°K. The positive results of ΔH* in Table 1 suggest that steel dissolving in HCl is an endothermic process. The negative values of -ΔS* are more significant in the presence of MME than the blank solution, indicating that competitive adsorption of MME replaces water molecules on the MS surface. The decrease in the -ΔS* value is associated with the rise in MME concentration, which aids in creating an anti-corrosive layer or protective film on the MS surface through MME molecules. The activation energy (Ea) required for the formation of corrosion products was determined by analyzing the slope (-Ea / 2.303R) of the Arrhenius plot correlating Log CR with 1/T (Figure 2 (a)). The computed Ea values are listed in Table 2, where CR represents the corrosion rate, R denotes the gas constant, and T is the temperature measured in absolute units [29, 30]. Typically, the activation energy values are observed to rise following the introduction of MME, suggesting that MME has been physically adsorbed onto the MS surface.

The transition state equation evaluates the enthalpy and entropic parameters during corrosion (Eq. 5) [30].

$$C_R = \frac{RT}{hN}\exp\left(\frac{\Delta S^*}{R}\right)\exp\left(-\frac{\Delta H^*}{R}\right) \qquad (5)$$

A represents the frequency factor, Ea stands for the activation energy, R is the gas constant, T denotes the absolute temperature, h symbolizes Planck's constant, and N represents Avogadro's number. Fig. 2 (b) displays a log (Cr / T) graph vs 1/ T. The values for enthalpy of activation and entropy of activation are determined from the slope (-ΔH/ 2.303 R) and intercept log (R/ Nh) + (ΔS / 2.303 R) of the linear plots and are reported in Table 2.

The results showed that the enthalpy (ΔH) values for the dissolving process of MS were more significant in the presence of inhibitors compared to when they were absent. The

positive numbers suggest that dissolving mild steel is an endothermic process, indicating that mild steel is resistant to dissolution. When $\Delta S^* < 0$, it shows that the adsorption process was sluggish, and the creation of complex compounds was linked to the rate-determining step, resulting in a reduction in disorder following the synthesis of the complex compound.

It is evident from the above graphs the inhibition rate is at its lowest 200ppm concentration and maximum at 1000 ppm concentration because of the increase in Enthalpy of the MME, and even the rise in temperature or immersion time has the most negligible effect on the corrosion inhibition by change in Ionisation Energy of the organic compound; this is the sequel of secondary and tertiary Hydrogen bonding of organic molecules side chains and functional groups.

3.1.2. Adsorption isotherms:

Different isotherms were investigated to judge the nature of the substituted adsorption process of MME on metal surfaces. One such is Langmuir isotherm, from which we can procure significant variables of synergy between the metal surface and inhibitor. The correlation between the fraction of metal surface blocked by inhibitor and inhibitor concentration was given by the equation (Eq. 6),

$$\frac{C}{\theta} = \frac{1}{K_{ads}} + C \qquad (6)$$

K_{ads} is the inhibitor adsorption process constant, θ is the fraction of the metal surface blocked by the inhibitor, and C is the inhibitor concentration. A linear plot obtained between C/θ vs C (Fig. 2 (c)) having a correlation coefficient near to unity for different concentrationsof MME at 35°C employing the gravimetric method was studied. From the intercept lines on the C/θ axis, K_{ads} values are calculated and listed in Table 2. The correlation coefficients were very close to 1 (R^2>0.95).This performance shows that the adsorption of inhibition of the mild steel surface in a 1 M HCl solution followed the standard free energy of adsorption, ΔG_{ads} were calculated using the following relationship (Eq. 7) [14]:

$$\Delta G_{ads} = -RT \ln\left(1\times10^{6} K_{ads}\right) \qquad (7)$$

Where 1×10^6 is the concentration of water molecules expressed in mL/L, R is the universal gas constant, and T is the temperature in Kelvin. The Gibbs - Helmholtz equation was used to calculate the thermodynamic parameters enthalpy and entropy of adsorption (ΔH_{ads} and ΔS_{ads}) (Eq. 8) [31].

$$\Delta G_{ads} = \Delta H_{ads} - T\Delta S_{ads} \quad (8)$$

The calculated values of ΔH_{ads} ΔS_{ads} ΔG_{ads} K_{ads} are listed in Table 3.The different types of adsorption processes, whether physical or chemical, are predicted from the value of ΔH_{ads} [32]. It is proposed that negative ΔG_{ads} Values between 20 kJ/mol and 40 kJ/mol imply a mixed inhibition process. At higher temperatures, the K_{ads} Value reduces, suggesting physical adsorption of inhibitor. Also, negative ΔH_{ads} values less than 40 kJ/mol exhibit exothermic reactions and the physiologic sorption of organic molecules on metal surfaces, further confirming the weight loss method results [31]. K_{ads} indicates the strength of interaction between the adsorbable and sorbent. The greater the values of K, the larger the adsorption efficiency. The low value of K_{ads} (1.70) in the present study showed a weak interaction between the inhibitor and the mild steel surface at that temperature.

3.2. Electrochemical Measurements

Figure 3 displays PDP curves, Nyquist plots, Bode diagrams, and Phase angle curves photographs of the impedance data. Both inhibitor-free and inhibitor-containing electrolytes displayed a semi-circular impedance plot on the graph, suggesting that the charge transfer rate influences mild steel corrosion under acidic conditions [33] Figure 3(b) shows a rise in the diameter of the semicircle. Higher inhibitor concentration (in ppm) increases electrical resistance at the electrolyte contact, resulting in a reduced corrosion rate. The Nyquist semicircles were used to compute and tabulate the Double-layer capacitance (C_{dl}) and Charge transfer resistance (R_{ct}) in Table 4. Increasing inhibitor concentration as C_{dl} decreases ensures an elevation in the electrical double layer at the electrolyte interface. The inhibitor efficiency (IE%) increased as the inhibitor concentration rose, as shown in Table 4. A single time constant was seen in Bode plots (Figure 3(c)) only for specific inhibitor doses. The protective adsorption layer development was enhanced due to an increased phase angle (Figure 3(d)). Higher concentration leads to increased adsorption of inhibitor molecules onto electrolytes, which reduces the metal dissolution rate. Figure 3(a) depicts the impact of different concentrations of MME on the anionic and cathodic polarization of mild steel in 1M HCl. The Tafel lines for electrolytes with and without inhibitors were parallel, indicating that the inhibitor unaffected the corrosion process. Kinetic parameters, including Corrosion potential (E_{corr}), Current density (i_{corr}), anodic slopes (β_a), and cathodic slopes (β_c), were determined from the plot and listed in Table 3. Introducing MME to the corrosive solution resulted in a decreased corrosion current density with minimal impact on the corrosion potential (E_{corr}).

Anodic control over the corrosion process was achieved compared to the unrestrained system, as shown by the change in E_{corr} values towards positive (less damaging) for anodic curves and negative (noble) for cathodic curves [25].

MME is rated as an inhibitor inhibiting mild steel and hydrogen dissolution and evolution. The inhibition efficiency is calculated using the equation (Eq. 9) [34]

$$\eta(\%) = \left(1 - \frac{i_{corr}}{i^{0}_{corr}}\right) \times 100 \qquad (9)$$

There are three different mechanisms of inhibition by organic molecules. The first mechanism is by conquering inhibitors on metal, thereby reducing the metal surface area exposed to the corrosion process [35]. The remaining two approaches are electro-catalytic and active site blocking effects, wherein inhibition occurs by activation of the energy barrier on anodic and cathodic reactions. It is observed that there is a progressive decrease and increase in I_{corr} and R_p values on the addition of MME, indicating the highest corrosion mitigation efficiency of 91.43 % at 1000ppm.

3.3. Surface analysis

3.3.1. UV -visible spectroscopic measurements

UV–visible spectra aid in comprehending MME's adsorption characteristics on mild steel (Figure 4a). The absorption peaks from the inhibitor and mild steel immersed in 1 M HCl with 600 ppm of MME extract for 6 hours at 35°C exhibit transitions at 300 nm and 400 nm. The absorbance values are approximately 2 and 0.7 for the test solution with MME in 1M HCl without the immersion of mild steel and 2.1 and 0.7 for MME-mediated inhibition of mild steel after immersion. Based on prior studies, changes in the highest absorbance peak value and its position indicate the development of a complex between released Fe^{2+} from steel and MME throughout the corrosion process. The phenomenon is caused by $\pi - \pi^*$ and n $- \pi^*$ transitions occurring across the complete conjugated structure of the carbonyl molecule in the inhibitor. This process is influenced by the electronic structure system of the MME and involves considerable charge transfer behaviour [36]. A blue shift, indicating a drop in wavelength and an increase in the frequency range, was seen at both absorbance peaks, indicating the development of a complex between Fe^{2+} and MME.

3.3.2. FTIR surface analysis

Plant extracts include several chemicals absorbed into the steel surface, enhancing its anti-corrosive qualities. The current research utilized FTIR analysis to examine the inhibitive

layer developed on the metal surface in the presence of MME and identify the functional groups of MME that interact with mild steel. FTIR analysis was conducted on mild steel and MME. The mild steel was immersed in a solution containing MME, and the resulting spectra are displayed in figure 4b(ii). The MS spectra showed a peak at 3269 cm^{-1} corresponding to O-H bending. The absorption peaks at 2883 cm^{-1}, 2360 cm^{-1}, 1716 cm^{-1}, 1312 cm^{-1}, and 1210 cm^{-1} correspond to C-H, O=C=O, C=O, phenolic stretching O-H, and C-O bond, respectively. The MME spectrum acknowledged that the peak at 3301 cm^{-1} represents the typical stretching vibration of the C-H group. The stretching vibration of the C-H bond was observed at2899 cm^{-1}. The stretching vibrations of O=C=O, C-H, and O-H bonds were observed at2344 cm^{-1}, 1484 cm^{-1}, and 1338 cm^{-1}, respectively. The data shows the existence of alkane, carboxylic acid, and hydroxyl groups in MME, which align with the structure of common anti-corrosive chemicals. The FT-IR spectra of the corrosion product on MS submerged in 1M HCL with an MME of 600ppm displays adsorption peaks at 3382 cm^{-1}, 2890 cm^{-1}, 2344 cm^{-1}, and 1480 cm^{-1}, corresponding to the stretching vibrations of O-H, C-H, O=C=O, and C-H bonds, respectively. The comparison between the MME/MS spectrum and MS spectra alone indicates that bonds such as C=O and C-O have gone, suggesting that these bonds are coordinated with other MME to create an MME+Fe^{+2} film on MS. Some FTIR absorption peaks of the MME/MS complex moved to shorter wave numbers, whereas others shifted to longer wave numbers. The FTIR spectrum of the MME/MS complex displayed all the distinctive bands found in the individual IR spectra of MS and MME. The findings indicate that MME was adsorbed onto the surface of MS, as shown in Figure (4b(iii))[36,37].

3.3.3. SEM analysis

A scanning electron microscope (SEM) investigation examined the surface structure of a mild steel sample immersed in acid solutions with and without inhibitors. Figure 5 (a) shows a smooth, mild steel surface without defects. Figure 5 (b) illustrates the surface structure of mild steel exposed to 1 M HCl for 12 hours, resulting in severe corrosion. The image shows grain boundaries between ferrite and perlite where iron oxide/oxyhydroxide deposits form and extend to other areas. Corrosion inhibitors help protect metal surfaces from corrosion by acidic solutions. An optimal concentration of 600 ppm of MME effectively prevents corrosion. Figure 5 (c) displays a pristine surface with fewapparent imperfections. The MS sample has a uniform, sleek surface with a high-quality protective coating [38,39].

3.4. Quantum chemical analysis

The efficacy of MME inhibition has been associated with quantum chemical characteristics, namely the energy levels of HOMO, LUMO and the energy gap between them. According to the frontier molecular orbital theory, electron transition occurs due to the contact between the highest occupied molecular orbital (HOMO) and the lowest unoccupied molecular orbital (LUMO) of the reacting species. The energy of the Highest Occupied Molecular Orbital (HOMO) reflects the molecule's vulnerability to electrophilic assault, which is connected to the ionization potential. The energy of LUMO indicates the molecule's vulnerability to nucleophilic assault, linked to electron affinity [18].

Figure 6. displays the analyzedcompounds' optimized molecular structure and electronic density distribution. Table 5shows the acquired energy levels of the Highest Occupied Molecular Orbital (HOMO) and Lowest Unoccupied Molecular Orbital (LUMO). The molecule's electron-accepting capability rises as the E_{LUMO} value decreases. An immense E_{HOMO} value suggests a greater capacity of an inhibitor to transfer an electron from its p-orbital to the vacant d-orbital of the electrophile or steel surface [11]. A minor energy difference between the Highest Occupied Molecular Orbital (HOMO) and the Lowest Unoccupied Molecular Orbital (LUMO) results in improved inhibitory effectiveness of the inhibitor. The observations align with the FTIR data, indicating the carbonyl group's existence coordinated with the metal surface. Cis-vaccenic acid, with an E_{HOMO} of -6.097eV and an E_{LUMO} of -0.346eV, is more suitable for corrosion inhibition due to its electron density distribution. The inhibitor's reactivity and stability are evaluated using the energy gap (ΔE) [35]. The ΔE value for cis-vaccenic acid is 6.20 electron volts, lower than other components in MME. The inhibitor's reactivity and stability are assessed using Absolute hardness (η) and resistance to deformation. Higher inhibitory efficiency is achieved with a lower ΔE value [37]. The results indicate that the MME has a positive effect on corrosion mitigation.

3.5. Inhibition Mechanism

The interface between the corrosion solution and metal is active in free acid solutions. Still, when the green inhibitor MME was added, the active state altered to a passive state, causingthe adsorption of the inhibitor molecule. Plant extract components in acidic environments actas neutral molecules or cations and are adsorbed through physical or chemical methods. Inphysisorption, the anions of HCl get adsorbed on MS to make it a cathode, and then, secondly, the protonated molecules from the inhibitor are adsorbed on the metal surface.The chemisorption process is detailed below in an equation,

$$Fe + MME \longleftrightarrow Fe(MME)_{ads}$$

$$Fe(MME)_{ads} \longleftrightarrow Fe^{2+} + MME + ne^{-}$$

$$MME_{aq} + H_2O_{ads} \longleftrightarrow MME_{ads} + H_2O_{aq}$$

A Quantum chemical study of *Mukia maderaspatana* extract identified the presence of cis-vaccenic acid, linoelaidic acid, and n-Hexadecanic acid. The anti-corrosive activity of green inhibitors is derived from the synergistic impact of many phytochemical components in plant extracts through adsorption. Cis-vaccenic acid demonstrates superior anti-corrosive capabilities compared to the other two components due to its high E_{HOMO} value of -6.097eV and low E_{LUMO} value of -0.346eV in the aqueous phase, as shown in Table 6. Another significant element is the energy gap, ΔE, which influences the reactivity of molecules towards adsorption. As the ΔE value falls, the molecule's inhibitory effectiveness improves, and vice versa. When placed in a 1 M HCl solution, the phytochemical components of *Mukia maderaspatana* extract undergo protonation at their heteroatom sites; this makes it difficult for them to be adsorbed onto the electrode surface because steel becomes positively charged in the presence of HCl. The chloride ions in the solution are readily adsorbed onto the metal surface, forming negatively charged iron-chloride species on the metal surface. The molecules in the extract adhere to the surface of MS, creating a physical barrier that reduces the corrosive impact of the acidic environment, as seen by the FTIR analysis [38,39].

4. Conclusion

This study assessed the effectiveness of *Mukia maderaspatana* plant extract in reducing corrosion on MS in 1 M HCl using weight loss analysis, ac impedance, DC polarization tests, and surface analysis. The results obtained are pretty consistent. The inhibitor efficiency achieved by weight loss, EIS investigations, and polarization measurements is 93%, 86%, and 91% for MME concentrations of 1000 ppm, respectively. The inhibitor's adsorption is exothermic spontaneous and adheres to Langmuir's adsorption isotherm. Impedance experiments showed that corrosion decreased as charge transfer resistance increased. The Tafel plots indicated that MME has a mixed kind of inhibition. UV analysis verifies the formation of a complex between the inhibitor and Fe2+. FTIR analysis verified the adsorption of reducing sugar. SEM examination clearly showed the green inhibitor's creation of a protective layer, indicating that MME is an effective environmentally friendly inhibitor for preventing corrosion of mild steel in a harsh acid environment.

Acknowledgement:

The authors thankthe Principal and Head of the Industrial Biotechnology Department at the Government College of Technology, Coimbatore, for facilitating this research.

Reference

1. Lin, B. and Zuo, Y. "Corrosion inhibition of carboxylate inhibitors with different alkylene chain lengths on carbon steel in an alkaline solution" ,*RSC Advances*, **9**(13), pp. 7065–7077 (2019).DOI:10.1039/C8RA10083G
2. Haque, J., Srivastava, V., Verma, C., et al. "N-Methyl-N, N, N-trioctylammonium chloride as a novel and green corrosion inhibitor for mild steel in an acid chloride medium: electrochemical, DFT and MD studies" ,*New Journal of Chemistry*, **41**(22), pp. 13647-13662 (2017).DOI:10.1039/C7NJ02254A
3. El Faydy, M., Touir, R., Touhami, M.E., et al. "Corrosion inhibition performance of newly synthesized 5-alkoxymethyl-8-hydroxyquinoline derivatives for carbon steel in 1 M HCl solution: experimental, DFT and Monte Carlo simulation studies" ,*Physical Chemistry Chemical Physics*, **20**(30), pp. 20167-20187 (2018).DOI:10.1039/C8CP03226B
4. Rizi, A., Sedik, A., Acidi, A., et al. "Sustainable and Green Corrosion Inhibition of Mild Steel: Insights from Electrochemical and Computational Approaches" ,*ACS omega*, **8**(49), pp. 47224-38 (2023). DOI:10.1021/acsomega.3c06548
5. Sukul, D., Pal, A., Saha, S.K., et al. "Newly synthesized quercetin derivatives as corrosion inhibitors for mild steel in 1 M HCl: combined experimental and theoretical investigation" ,*Physical Chemistry Chemical Physics*, **20**(9), pp. 6562-6574 (2018).DOI:10.1039/C7CP06848D
6. Sliem, M.H., Afifi, M., Bahgat Radwan, A., et al. "AEO7 surfactant as an eco-friendly corrosion inhibitor for carbon steel in HCl solution" ,*Scientific reports*, **9**(1), pp. 1-16 (2019).DOI:10.1038/s41598-018-37254-7
7. Fazal, B.R., Becker, T., Kinsella, B., et al. "A review of plant extracts as green corrosion inhibitors for CO2 corrosion of carbon steel" ,*NPJ Materials Degradation*, ***6***(1), pp. 5 (2022). DOI:10.1038/s41529-021-00201-5
8. Medupin, R.O., Ukoba, K.O., Yoro, K.O., et al. "Sustainable approach for corrosion control in mild steel using plant-based inhibitors: A review" ,*Materials Today Sustainability*, ***22***, pp. 100373 (2023). DOI:10.1016/j.mtsust.2023.100373
9. Zakeri, A., Bahmani, E. and Aghdam, A.S.R. "Plant extracts as sustainable and green corrosion inhibitors for protection of ferrous metals in corrosive media: A mini

review" ,*Corrosion Communications*, ***5***, pp. 25-38 (2022). DOI:10.1016/j.corcom.2022.03.002

10. de Souza Morais, W.R., da Silva, J.S., Queiroz, N.M.P., et al. "Green corrosion inhibitors based on plant extracts for metals and alloys in corrosive environment: a technological and scientific prospection", *Applied Sciences*, ***13***(13), pp. 7482 (2023). DOI:10.3390/app13137482
11. Marhamati, F., Mahdavian, M. and Bazgir, S. "Corrosion mitigation of mild steel in hydrochloric acid solution using grape seed extract" ,*Scientific reports*, ***11***(1), pp. 18374 (2021). DOI:10.1038/s41598-021-97944-7
12. Dagdag, O., Safi, Z., Hsissou, R., et al. "Epoxy pre-polymers as new and effective materials for corrosion inhibition of carbon steel in acidic medium: Computational and experimental studies" ,*Scientific reports*, **9**(1), pp. 1-14 (2019).DOI:10.1038/s41598-019-48284-0
13. Krishnaveni, K., Ravichandran, J., and Selvaraj, A. "Effect of *Morinda tinctoria* leaves extract on the corrosion inhibition of mild steel in acid medium" ,*Acta MetallurgicaSinica (English Letters)*, **26**(3), pp. 321-327 (2013).DOI:10.1007/s40195-012-0219-9
14. Mobin, M., Basik, M., and Aslam, J. "Pineapple stem extract (Bromelain) as an environmental friendly novel corrosion inhibitor for low carbon steel in 1 M HCl" ,*Measurement*, **134**, pp. 595-605 (2019).DOI:10.1016/j.measurement.2018.11.003
15. Li, D., Zhang, P., Guo, X., et al. "The inhibition of mild steel corrosion in 0.5 M H_2SO_4 solution by radish leaf extract" ,*RSC Advances*, **9**(70), 40997-41009 (2019).DOI:10.1039/C9RA04218K
16. Al Otaibi, N. and Hammud, H.H. "Corrosion Inhibition Using Harmal Leaf Extract as an Eco-Friendly Corrosion Inhibitor" ,*Molecules*, **26**(22), pp. 7024 (2021).DOI:10.3390/molecules26227024
17. Gomathy, G., Vijay, T., Sarumathy, K., et al. "Phytochemical screening and GC-MS analysis of mukiamaderaspatana (L.) leaves" ,*Journal of Applied Pharmaceutical Science*,**2**(12), pp. 104-106 (2012).DOI:10.3390/10.7324/JAPS.2012.21220
18. Mobin, M. and Rizvi, M. "Adsorption and corrosion inhibition behavior of hydroxyethyl cellulose and synergistic surfactants additives for carbon steel in 1 M HCl" , *Carbohydrate polymers*, **156**, pp. 202-214 (2017).DOI:10.1016/j.carbpol.2016.08.066

19. Deyab, M.A., Zaky, M.T. and Nessim, M. I. “Inhibition of acid corrosion of carbon steel using four imidazolium tetrafluoroborates ionic liquids” , *Journal of Molecular Liquids,* **229**, pp. 396-404(2017).DOI:10.1016/j.molliq.2016.12.092
20. Dehghani, A., Bahlakeh, G., Ramezanzadeh, B., et al. “A combined experimental and theoretical study of green corrosion inhibition of mild steel in HCl solution by aqueous Citrulluslanatus fruit (CLF) extract” ,*Journal of Molecular Liquids,* **279**, pp. 603-624 (2019).DOI:10.1016/j.molliq.2019.02.010
21. Rabizadeh,T. and Asl, SK. “Casein as a natural protein to inhibit the corrosion of mild steel in HCl solution” , *Journal of Molecular Liquids,* **276**, pp. 694-704 (2019).DOI:10.1515/corrrev-2021-0101
22. Alibakhshi, E., Ramezanzadeh, M., Haddadi, S.A., et al. “Persian Liquorice extract as a highly efficient sustainable corrosion inhibitor for mild steel in sodium chloride solution” ,*Journal of cleaner production.,* **210**, pp. 660-672 (2019).DOI:10.1016/j.jclepro.2018.11.053
23. Abdelaziz, S., Benamira, M., Messaadia, L., et al. “Green corrosion inhibition of mild steel in HCl medium using leaves extract of Arbutus unedo L. plant: An experimental and computational approach” ,*Colloids and Surfaces A: Physicochemical and Engineering Aspects.*, **619**, pp. 126496 (2021).DOI:10.1016/j.colsurfa.2021.126496
24. Khan, P.F., Shanthi, V., Babu, R.K., et al. “Effect of benzotriazole on corrosion inhibition of copper under flow conditions” , *Journal of Environmental Chemical Engineering*, **3**(1), pp. 10-19 (2015).DOI:10.1016/j.jece.2014.11.005
25. Okon Eddy, N., Odiongenyi, A.O., Ebenso, E.E., et al. “Plant Wastes as alternative sources of sustainable and green corrosion inhibitors in different environments” ,*Corrosion Engineering, Science and Technology*, ***58***(5), pp. 521-533 (2023). DOI:10.1080/1478422X.2023.22042
26. Hegazy, M.A. and Atlam, F.M. “Three novel bolaamphiphiles as corrosion inhibitors for carbon steel in hydrochloric acid: Experimental and computational studies” , *Journal of Molecular Liquids,* **218**, pp. 649-662 (2016).DOI:10.1016/j.molliq.2016.03.008
27. Alkhathlan, H.Z., Khan, M., Abdullah, M.M.S., et al. “Anti-corrosive assay-guided isolation of active phytoconstituents from *Anthemispseudocotula* extracts and a detailed study of their effects on the corrosion of mild steel in acidic media” , *RSC Advances*, **5**(67), pp. 54283-54292 (2015).DOI:10.1039/C5RA09154C

28. Krishnaveni, K., Ravichandran, J. and Selvaraj, A. “Inhibition of mild steel corrosion by *Morinda tinctoria* leaves extract in sulphuric acid medium” , *Ionics*, **20**(1), pp. 115-126 (2014).DOI:10.1007/s11581-013-0954-6
29. Verma, C., Quraishi, M.A., Ebenso, E.E., et al. “3-Amino alkylated indoles as corrosion inhibitors for mild steel in 1M HCl: Experimental and theoretical studies” ,*Journal of Molecular Liquids*, **219**, pp. 647-660(2016).DOI:10.1016/j.molliq.2016.04.024
30. Geethamani, P., Narmatha, M., Dhanalakshmi, R., et al. “Corrosion inhibition and adsorption properties of mild steel in 1 M hydrochloric acid medium by expired ambroxol drug” , *Journal of Bio-and Tribo-Corrosion*, **5**(1), pp. 1-18 (2019).DOI:10.1007/s40735-018-0205-5
31. Abbout, S., Zouarhi, M., Chebabe, D., et al. “Galactomannan as a new bio-sourced corrosion inhibitor for iron in acidic media” , *Heliyon*, **6**(3), pp. e03574 (2020).DOI:10.1016/j.heliyon.2020.e03574
32. Mohammadinejad, F., Zandi, M.S., Bahrami, M.J., et al. “Metoprolol: New and Efficient Corrosion Inhibitor for Mild Steel in Hydrochloric and Sulfuric Acid Solutions” , *Acta ChimicaSlovenica*, **67**(3), pp. 710-719 (2020).DOI:10.17344/acsi.2019.5301
33. Prabakaran, M., Kim, S.H., Sasireka, A., et al. “*Polygonatumodaratum*extract as an eco-friendly inhibitor for aluminum corrosion in acidic medium” , *Journal of adhesion science and Technology*, **32**(18), pp. 2054-2069 (2018).DOI:10.1080/01694243.2018.1462947
34. Abd El-Lateef, H.M. “Experimental and computational investigation on the corrosion inhibition characteristics of mild steel by some novel synthesized imines in hydrochloric acid solutions” ,*Corrosion Science*, **92**, pp. 104-117 (2015).DOI:10.1016/j.corsci.2014.11.040
35. Khaled, K.F. and El-Maghraby, A. “Experimental, Monte Carlo and molecular dynamics simulations to investigate corrosion inhibition of mild steel in hydrochloric acid solutions” , *Arabian Journal of Chemistry*, **7**(3), pp. 319-326 (2014).DOI:10.1016/j.arabjc.2010.11.005
36. Hachani, S.E., Necira, Z., Mazouzi, D., et al. “Understanding the inhibition of mild steel corrosion by dianilineschiff bases: A DFT investigation” ,*Acta ChimicaSlovenica*, **65**(1), pp. 183-190 (2018).DOI:10.17344/acsi.2017.3803

37. Khaled, K.F. “Studies of iron corrosion inhibition using chemical, electrochemical and computer simulation techniques” , *Electrochimica Acta,* **55**(22), pp. 6523-6532 (2010).DOI:10.1016/j.electacta.2010.06.027
38. Božović, S., Martinez, S. and Grudić, V. “A novel environmentally friendly synergistic mixture for steel corrosion inhibition in 0.51 M NaCl” , *Acta ChimicaSlovenica,* **66**(1), pp. 112-122 (2019).DOI:10.17344/acsi.2018.4702
39. Sen, A. and Kumar, M. “Green approaches towards inhibition of corrosion in metals: A review”, In *AIP Conference* Proceedings, **2986**,(1) pp. 020027 (2024). AIP Publishing. DOI:10.1063/5.0198019

Figure captions

Figure 1. (a)Scopus database document count on the theme; and (b)Research Map on the theme

Figure 2. (a) Arrhenius plot, (b) Transition state plot, (c) Langmuir adsorption isotherm for MS immersed in 1 M HCl in the presence and absence of different concentrations of MME.

Figure 3. (a) PDP curves, (b) Nyquist plots, (c) Bode diagrams, (d) Phase angle curves for MS immersed in 1M HCl in the presence and absence of different concentrations of MME.

Figure 4. (a) UV- visible spectra of 1M HCl with (i) 600 ppm MME, (ii) MME + Fe^{2+} complex, (b) FT-IR for (i) MS (ii) MME (iii) MME/MS complex.

Figure 5. SEM images for MS (a) were polished, (b) exposed to 1M HCl solution, and (c) exposed to 1 M HCl solution containing 600 ppm MME for 12 h.

Figure 6. Results showing HOMO orbital, LUMO orbital, electrostatic potenial surface (ESP)in the aqueous phase

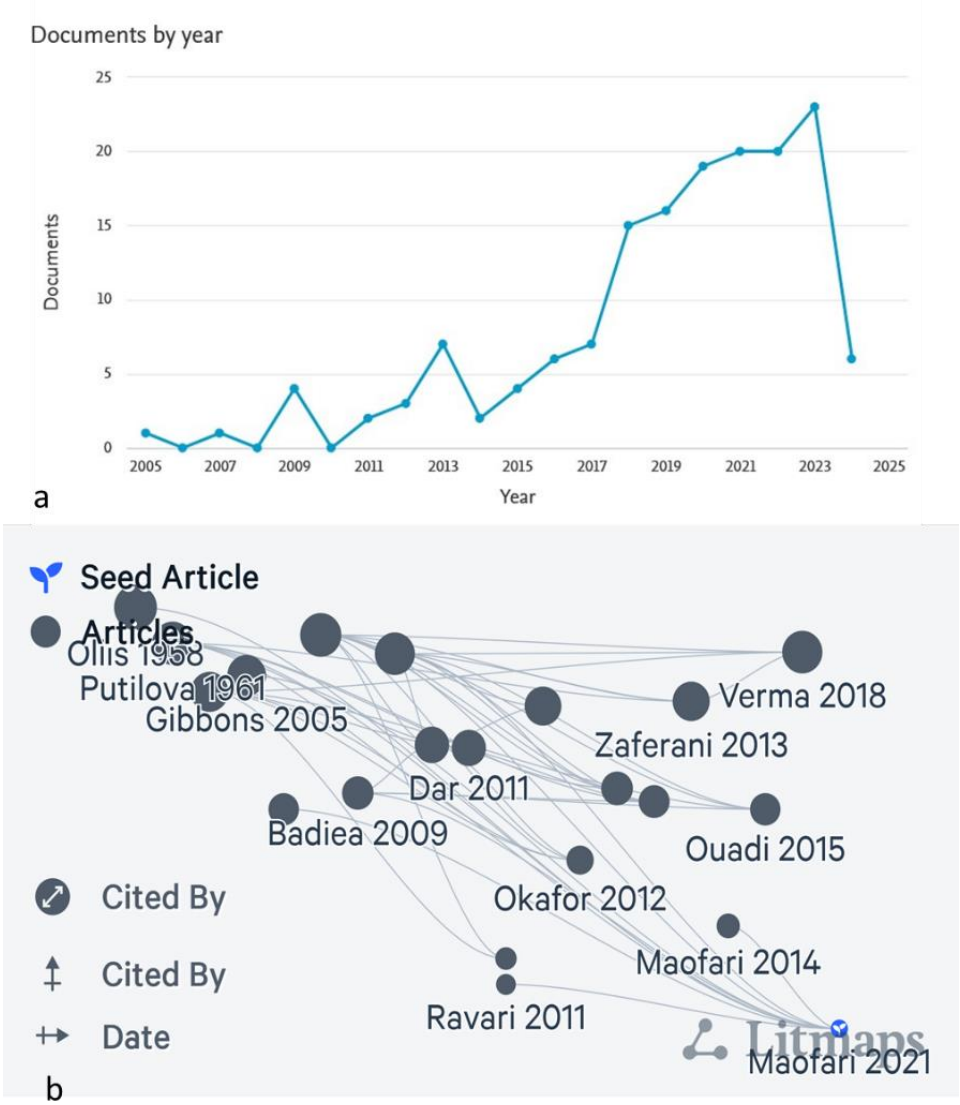

Figure 1. (a) Scopus database document count on the theme; and (b) Research Map on the theme

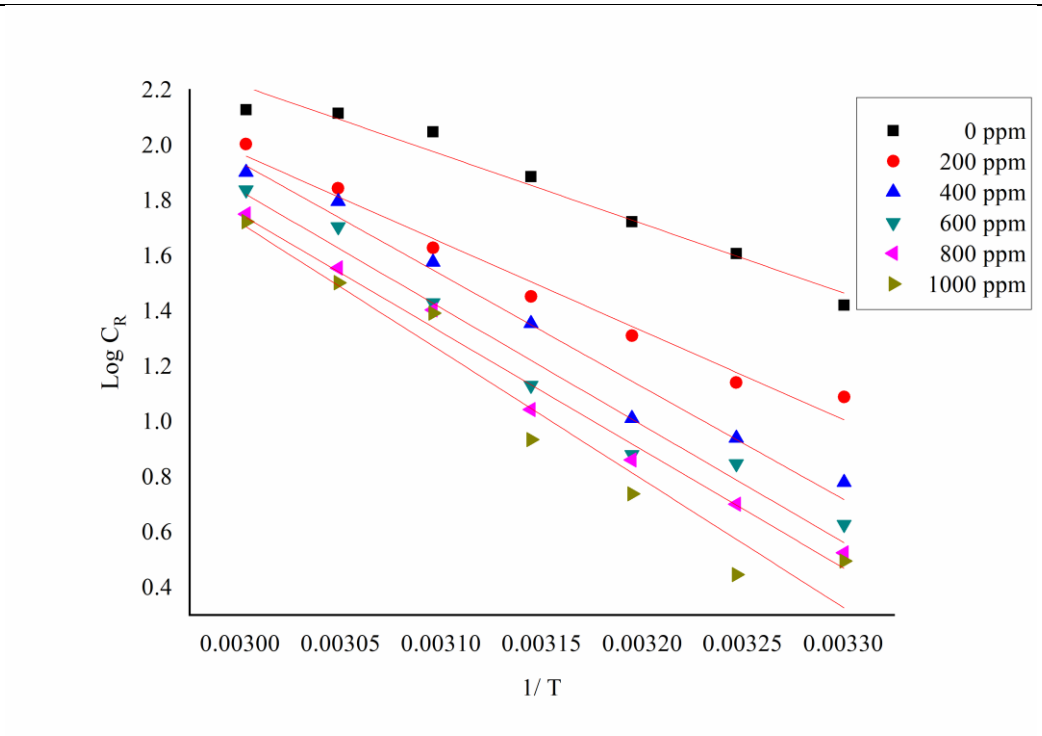
Log C_R
2.2
2.0
1.8
1.6
1.4
1.2
1.0
0.8
0.6
0.4
0.00300
0.00305
0.00310
0.00315
0.00320
0.00325
0.00330
1/ T
0 ppm
200 ppm
400 ppm
600 ppm
800 ppm
1000 ppm

(a)

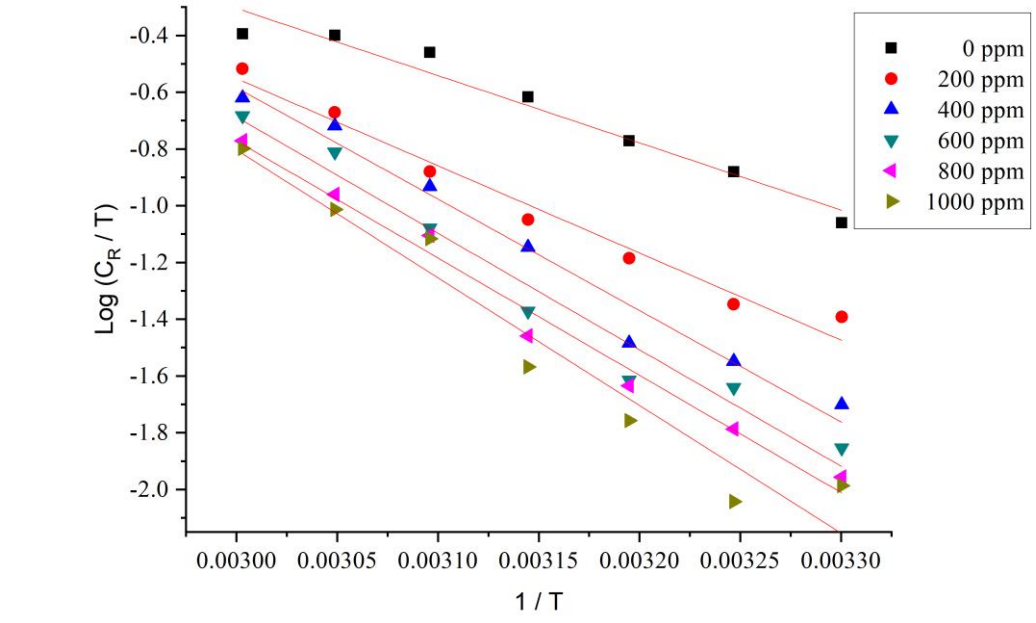
Log (C_R / T)
-0.4
-0.6
-0.8
-1.0
-1.2
-1.4
-1.6
-1.8
-2.0
0.00300
0.00305
0.00310
0.00315
0.00320
0.00325
0.00330
1 / T
0 ppm
200 ppm
400 ppm
600 ppm
800 ppm
1000 ppm

(b)

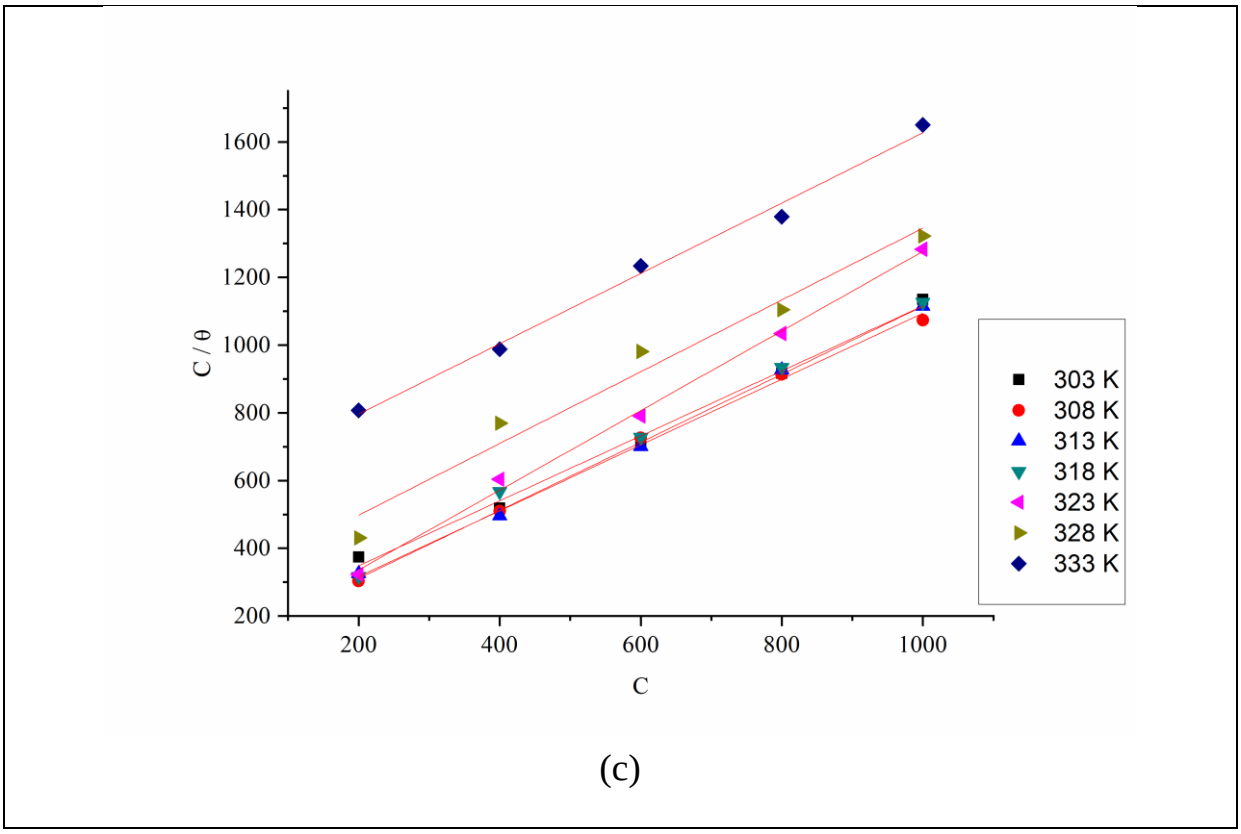

(c)

Figure 2. (a) Arrhenius plot, (b) Transition state plot, (c) Langmuir adsorption isotherm for MS immersed in 1 M HCl in the presence and absence of different concentrations of MME.

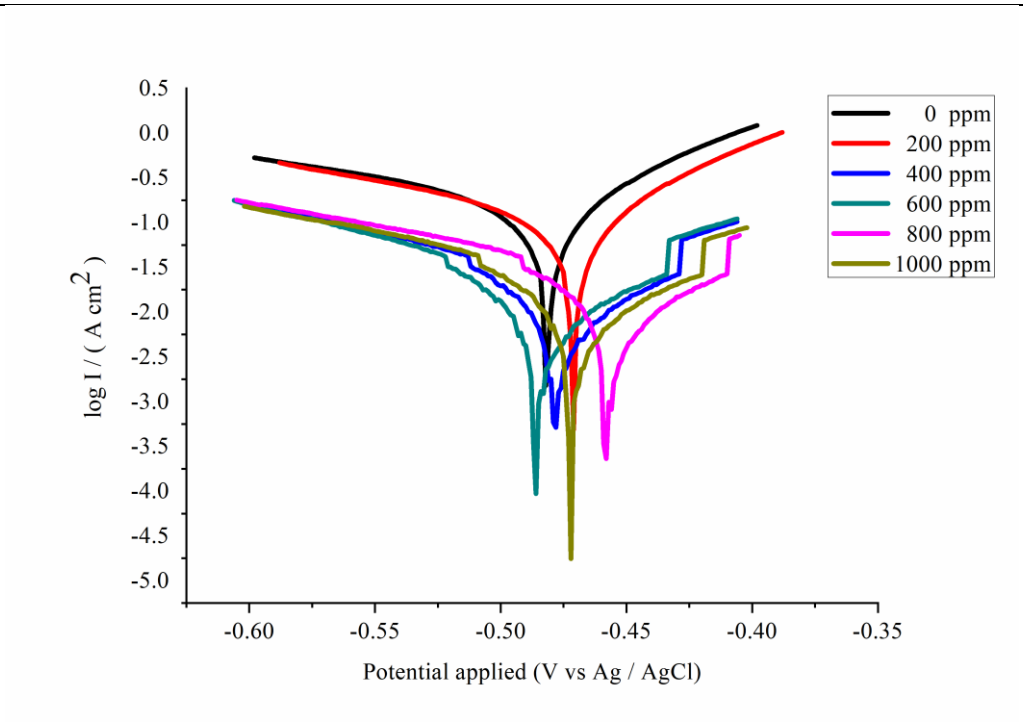
0 ppm
200 ppm
400 ppm
600 ppm
800 ppm
1000 ppm
log I / (A cm^2)
Potential applied (V vs Ag / AgCl)

(a)

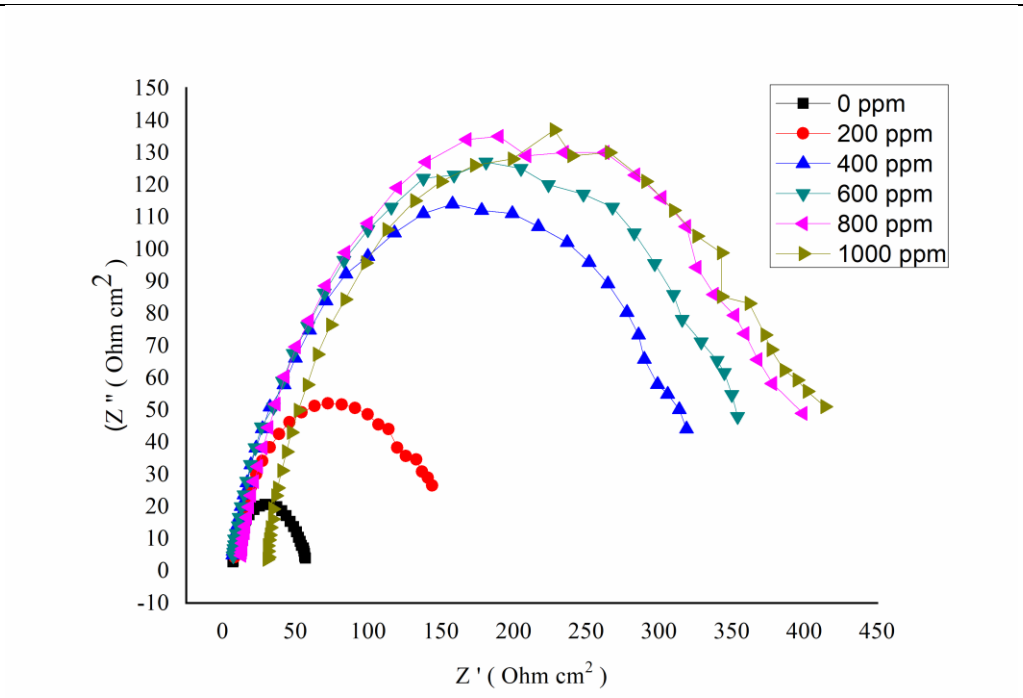
0 ppm
200 ppm
400 ppm
600 ppm
800 ppm
1000 ppm
(Z '' (Ohm cm^2)
Z ' (Ohm cm^2)

(b)

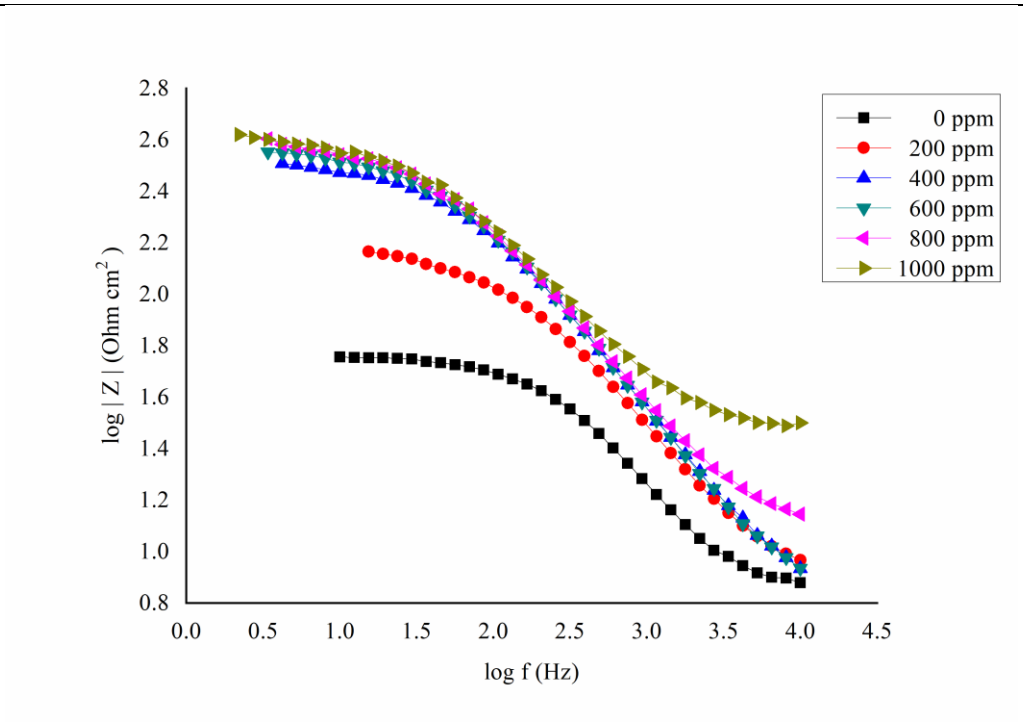

(c)

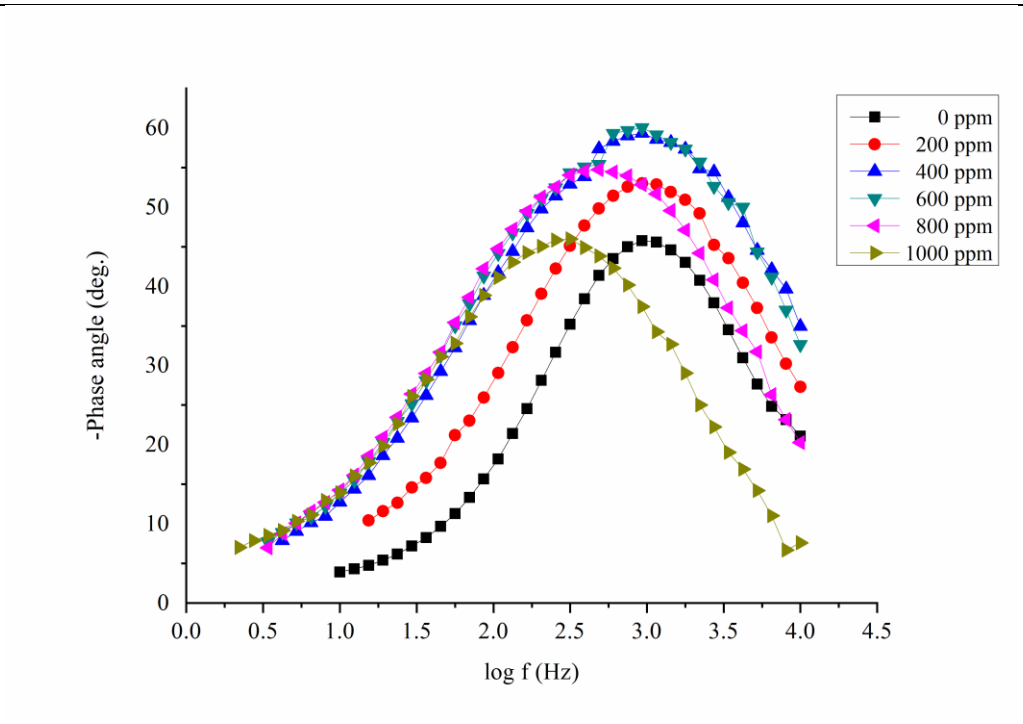

(d)

Figure 3. (a) PDP curves, (b) Nyquist plots, (c) Bode diagrams, (d) Phase angle curves for MS immersed in 1M HCl in the presence and absence of different concentrations of MME.

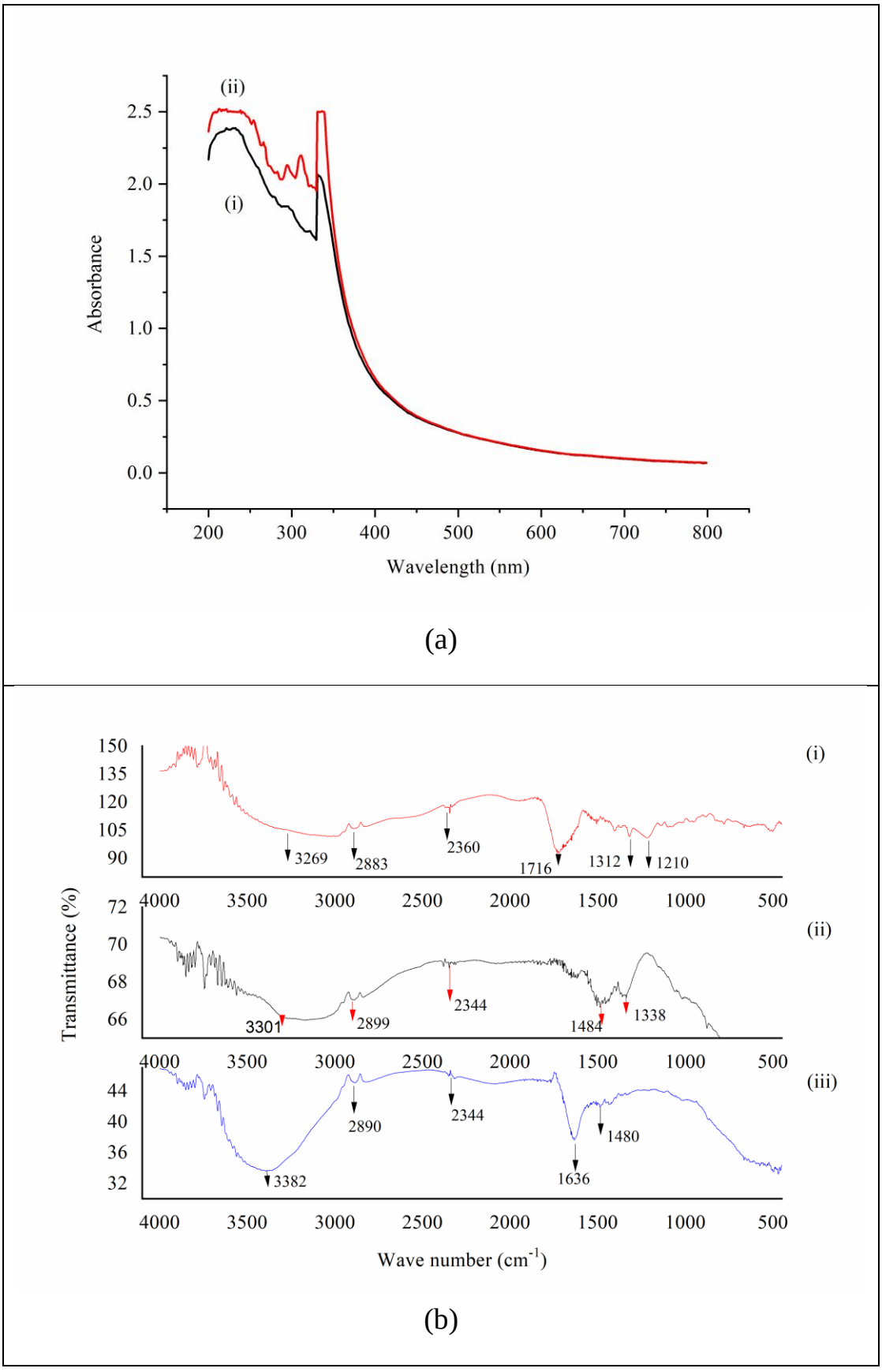

Figure 4. (a) UV- visible spectra of 1M HCl with (i) 600 ppm MME, (ii) MME + Fe^{2+} complex, (b) FT-IR for (i) MS (ii) MME (iii) MME/MS complex.

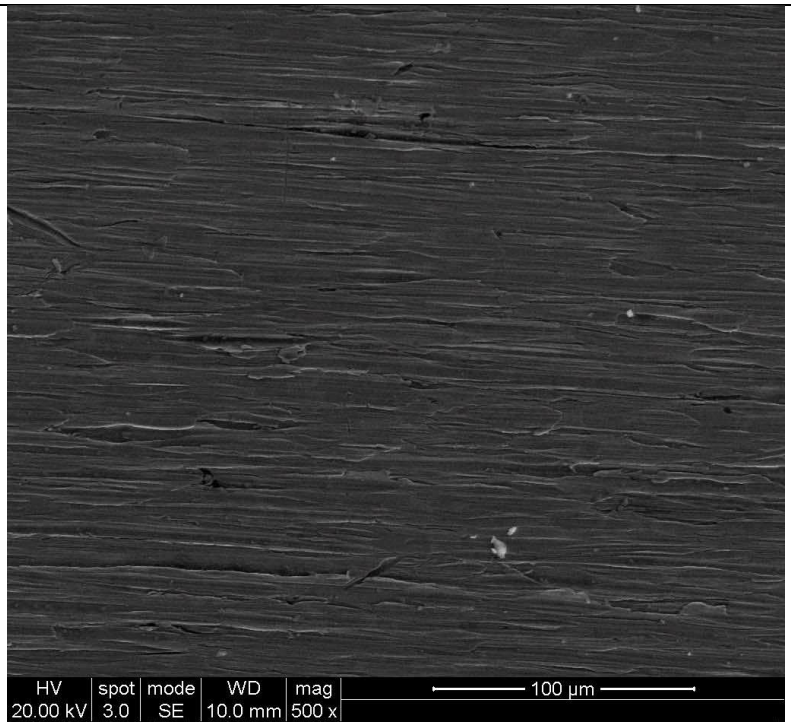
HV
20.00 kV
spot
3.0
mode
SE
WD
10.0 mm
mag
500 x
100 µm

(a)

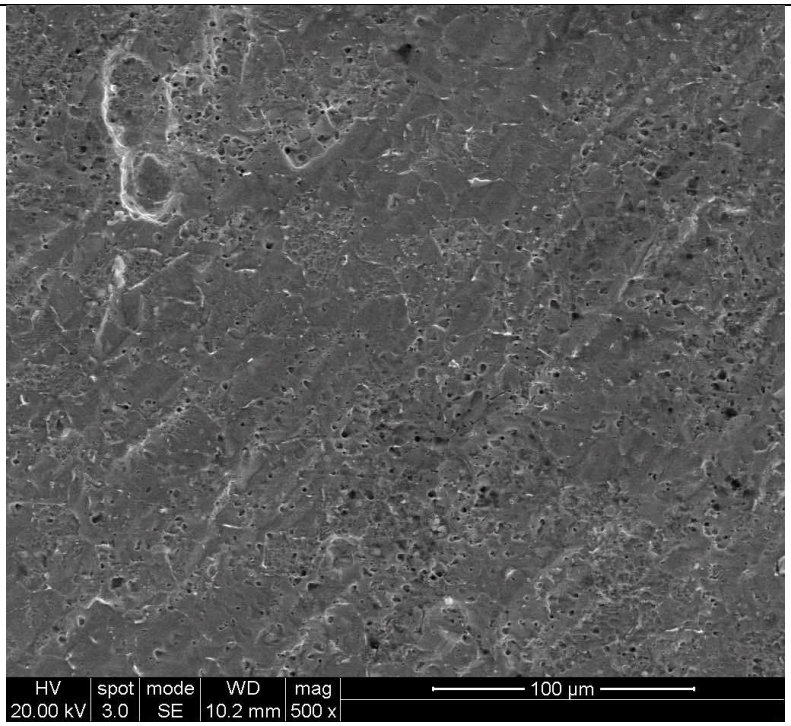
HV
20.00 kV
spot
3.0
mode
SE
WD
10.2 mm
mag
500 x
100 µm

(b)

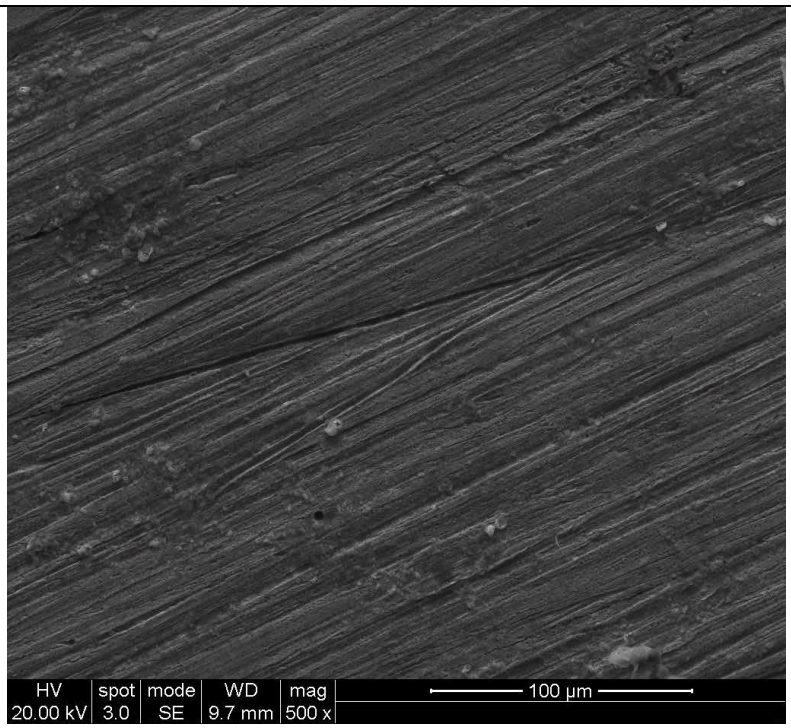

(c)

Figure 5. SEM images for MS (a) were polished, (b) exposed to 1M HCl solution, and (c) exposed to 1 M HCl solution containing 600 ppm MME for 12 h.

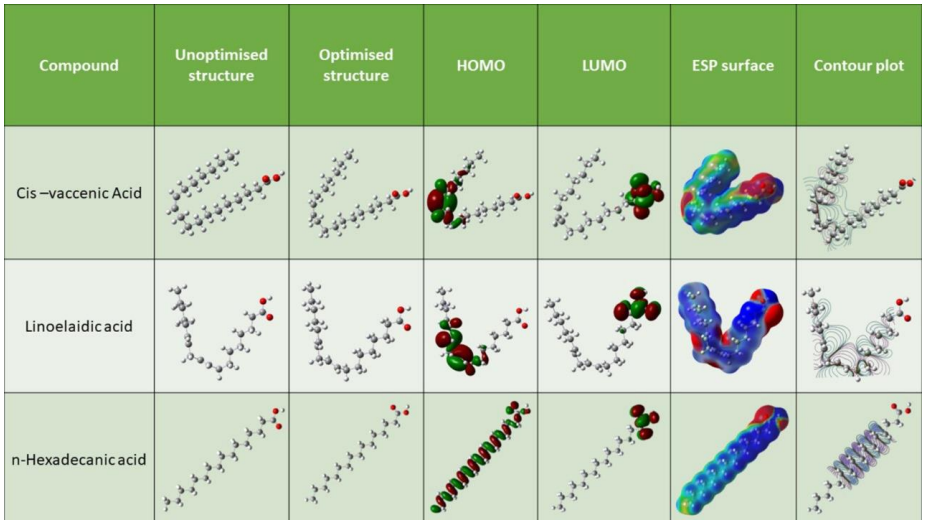

Figure 6. Results showing HOMO orbital, LUMO orbital, electrostatic potenial surface (ESP) in the aqueous phase

Table captions

Table 1. Activation parameters for MS in 1 M HCl in the presence and absence of different concentrations of MME

Table 2. Langmuir adsorption parameters and free energy of adsorption of MME as an inhibitor on the surface of mild steel

Table 3. Potentiodynamic polarization parameters for MS in 1 M HCl with and without different concentrations of MME

Table 4. Electrochemical impedance parameters for MS in 1 M HCl with and without different concentrations of MME

Table 5. Quantum chemical parameters of molecules from plant *Mukia maderaspatana* in aqueous phase

Table 1. Activation parameters for MS in 1 M HCl in the presence and absence of different concentrations of MME

MME Conc. (ppm)	Ea (kJ/mol)	ΔH* (kJ/mol)	-ΔS* (J mol/ K)
Blank	48.01	45.37	67.28
200	61.49	58.85	31.59
400	77.84	75.20	16.85
600	81.18	78.54	24.89
800	81.73	79.09	24.93
1000	88.82	86.18	45.57

Table 2. Langmuir adsorption parameters and free energy of adsorption of MME as an inhibitor on the surface of mild steel

Temp (K)	$-\Delta G°_{ads}$ (kJ mol^{-1})	K_{ads} (L/g)	$-\Delta H°_{ads}$ (kJ mol^{-1})	$-\Delta S°_{ads}$ (J mol^{-1} K^{-1})	R^2
303	22.07	6.39	38.35	0.054	0.96
308	23.07	8.19		0.051	0.99
313	24.72	9.09		0.047	0.99
318	24.48	7.21		0.047	0.99
323	24.7	9.87		0.042	0.99
328	22.25	3.5		0.049	0.97
333	20.59	1.7		0.053	0.99

Table 3. Potentiodynamic polarization parameters for MS in 1 M HCl with and without different concentrations of MME

MME Conc. (ppm)	Ecorr (mV), SCE	Icorr (µAcm-2)	βa (mVdec-1)	βc (mVdec-1)	Rp (Ωcm-2)	IE (%)
Blank	-474.3	124.2	70	184	177.6	0
200	-464.8	94.49	69	172	225.3	23.92
400	-421.2	19.63	57	190	972.7	84.19
600	-445.6	16.03	46	151	953.2	87.09
800	-453.3	13.74	43	134	1023	88.94
1000	-436.3	10.64	76	166	1361	91.43

Table 4. Electrochemical impedance parameters for MS in 1 M HCl with and without different concentrations of MME

MME Conc.(ppm)	Rs (Ω cm-2)	Rp (Ω cm-2)	Rct (Ω cm-2)	Cdl (µF cm-2)	IE (%)
Blank	8.34	46.5	38.16	12.3	0
200	13.4	122	108.6	10.1	64.86
400	22.3	275	252.7	9.1	84.9
600	29	284	255	8.71	85.04
800	24.2	307	282.8	8.66	86.51
1000	47.3	329	281.7	8.44	86.45

Table 5. Quantum chemical parameters of molecules from plant *Mukia maderaspatana* in aqueous phase

Compound Name	E-HOMO (eV)	E-LUMO (eV)	ΔE (eV)	Chemical Hardness (η)	Chemical potential (μ)	Electronegativity (χ)	Electrophilicity (ω)	Nucleophilicity (ε)
Cis-vaccenic acid	-6.097	-0.346	5.751	2.875	-3.222	3.222	1.805	0.553
Linoelaidic acid	-6.642	-0.34	6.301	3.15	-3.491	3.491	1.934	0.516
n-Hexadecanoic acid	-7.886	-0.339	7.547	3.773	-4.112	4.112	2.241	0.446

- **Vinayagam Rajasekar**, born on February 13, 1982, in Vellore, Tamil Nadu, India. He received his B.Tech and M.Tech in Biotechnology and Biopharmaceutical Technology from Anna University, Chennai, Tamil Nadu, India, in 2004 and 2006, is an Assistant Professor in the Department of Industrial Biotechnology at Government College of Technology, Coimbatore. With an illustrious career spanning 17 years in teaching, He has mentored and guided undergraduate students. His research interests include biological activity, molecular docking, nano metal oxides, adsorption, biocorrosion, nutraceutical production and published 7 International Journal papers.

- **Dr.M. Shyamala, M.Sc., M.Phil., Ph.D.,** Studied M.Sc., & M.Phil. Applied Chemistry at Avinashilingam Institute for Home Science and Higher Education for Women, Coimbatore and Ph.D. Chemistry at Anna University, Chennai, Tamil Nadu. Working as Professor & Head, Department of Chemistry, Government College of Engineering, Salem. Published 9 Papers in International Journals, Published 1 Book, Attended 17 Conferences & Seminars, Organised 12 training programmes, Attended 34 training programmes, Recipient of five World records from All India Book of Records, Recipient of 7 Awards, **Board of Governors** - State Government Nominee for Sri Sai Ram Engineering College, Chennai, **Academic Council** - University Nominee for P.S.R. Engineering College, Sivagasi & Excel Engineering College, Namakkal, **Awards Committee Chairman for** Central Polytechnic College, Tharamani, Chennai, **Expert Committee member of** The Tamil Nadu Dr. Ambedkar Law University, Chennai, **Board of Studies member of** Dr. N.G.P.Institute of Technology, Coimbatore and Murugappa Polytechnic College, Avadi. Visited Malaysia for a paper presentation and received Best Poster Award, Handled TEQIP World bank project and Attended Joint Review Mission meetings with World Bank, MHRD, NPIU (National Project Implementation Unit, Noida) & Other States SPFUs (State Project Facilitation Units), Life Member in ISTE. Looking after Tamil Nadu Engineering Admissions at Directorate of Technical Education, Chennai.

- **J Aravind** is a faculty of Biotechnology at Saveetha School of Engineering, Saveetha Institute of Medical and Technical Sciences, Saveetha University, Chennai. He received his PhD from the Vellore Institute of Technology in 2008; he has a teaching experience of 15 years and research experience of 20 years and has more than 70 publications in the field of Environmental Biotechnology. He is a regular peer reviewer for many Environmental Sciences and Engineering journals, for Elsevier and Springer Nature. He has served as an associate editor in prestigious journals. He is currently part of the international editorial board in Ecotoxicology and Environmental Safety, an Elsevier publication journal with an impact factor of 6.8.